

Increasing Anaerobic Acetate Consumption and Ethanol Yields in *Saccharomyces cerevisiae* with NADPH-Specific Alcohol Dehydrogenase

Brooks M. Henningsen, Shuen Hon,* Sean F. Covalla, Carolina Sonu, D. Aaron Argyros, Trisha F. Barrett, Erin Wiswall, Allan C. Froehlich,  Rintze M. Zelle

Mascoma LLC, Lebanon, New Hampshire, USA

Saccharomyces cerevisiae has recently been engineered to use acetate, a primary inhibitor in lignocellulosic hydrolysates, as a cosubstrate during anaerobic ethanolic fermentation. However, the original metabolic pathway devised to convert acetate to ethanol uses NADH-specific acetylating acetaldehyde dehydrogenase and alcohol dehydrogenase and quickly becomes constrained by limited NADH availability, even when glycerol formation is abolished. We present alcohol dehydrogenase as a novel target for anaerobic redox engineering of *S. cerevisiae*. Introduction of an NADPH-specific alcohol dehydrogenase (NADPH-ADH) not only reduces the NADH demand of the acetate-to-ethanol pathway but also allows the cell to effectively exchange NADPH for NADH during sugar fermentation. Unlike NADH, NADPH can be freely generated under anoxic conditions, via the oxidative pentose phosphate pathway. We show that an industrial bioethanol strain engineered with the original pathway (expressing acetylating acetaldehyde dehydrogenase from *Bifidobacterium adolescentis* and with deletions of glycerol-3-phosphate dehydrogenase genes *GPD1* and *GPD2*) consumed 1.9 g liter⁻¹ acetate during fermentation of 114 g liter⁻¹ glucose. Combined with a decrease in glycerol production from 4.0 to 0.1 g liter⁻¹, this increased the ethanol yield by 4% over that for the wild type. We provide evidence that acetate consumption in this strain is indeed limited by NADH availability. By introducing an NADPH-ADH from *Entamoeba histolytica* and with overexpression of *ACS2* and *ZWF1*, we increased acetate consumption to 5.3 g liter⁻¹ and raised the ethanol yield to 7% above the wild-type level.

Saccharomyces cerevisiae is the principal microorganism used to produce ethanol, of which 93 billion liters were globally produced in 2014 (1). However, new strains are needed for the production of second-generation biofuels. Pretreatment and monomerization of lignocellulosic substrates produce complex sugar mixtures, including the C₅ sugars xylose and arabinose that are poorly fermented by most wild-type *S. cerevisiae* strains (2, 3). In addition, a variety of inhibitory compounds are released, such as furfural, hydroxymethylfurfural, methylglyoxal, and acetate (4–6). It is therefore desirable not only to expand the substrate range of *S. cerevisiae* (3, 7–9) but also to increase its inhibitor tolerance (10–13).

Acetate is released during deacylation of hemicellulose and lignin and can be present in concentrations of >10 g liter⁻¹ in cellulosic hydrolysates (4, 14). At low pH particularly, this weak organic acid is a potent inhibitor of *S. cerevisiae* metabolism (15–17). Unfortunately, wild-type *S. cerevisiae* strains are poorly equipped to eliminate acetate from the medium under anoxic conditions. *S. cerevisiae* can grow on acetate as the sole carbon source under oxic conditions by converting acetate to acetyl coenzyme A (acetyl-CoA) with acetyl-CoA synthetase (ACS) (EC 6.2.1.1) and by either respiring acetyl-CoA in the tricarboxylic acid (TCA) cycle or upgrading acetyl-CoA to four-carbon intermediates in the glyoxylate pathway. However, succinate dehydrogenase, a central enzyme in the glyoxylate cycle, is part of the respiratory chain and does not function anaerobically. Unfavorable thermodynamics also prevent the conversion of acetate to ethanol via acetaldehyde through endogenous nonacetylating acetaldehyde dehydrogenase (ALDH) (EC 1.2.1.3–5) and alcohol dehydrogenase (ADH) (EC 1.1.1.1) (Fig. 1A).

Various metabolic engineering strategies have been devised to improve *S. cerevisiae*'s ability to anaerobically consume acetate. In 2010, Guadalupe Medina et al. pioneered the use of acetaldehyde

dehydrogenase (acetylating) (ADA) (EC 1.2.1.10) in *S. cerevisiae* (18), which opens up a thermodynamically favorable ATP-consuming route from acetate to ethanol via ACS, ADA, and ADH (Fig. 1B). The conversion of acetate to ethanol is not redox neutral and requires 2 NAD(P)H per acetate. Guadalupe Medina et al. chose to use the NADH-specific *mhpF* ADA from *Escherichia coli* and relied on endogenous ADH activity, which is predominantly NADH specific (19). In wild-type *S. cerevisiae* strains grown under anoxic conditions, surplus NADH generated during cellular growth is reoxidized via the production of glycerol, which thus plays an important role as an anaerobic “redox sink” (20, 21). By deleting the NADH-specific glycerol-3-phosphate dehydrogenase genes *GPD1* and *GPD2*, Guadalupe Medina et al. eliminated glycerol production and redirected the biosynthetic NADH surplus toward the conversion of acetate to ethanol.

The amount of surplus NADH generated during anaerobic growth of *S. cerevisiae* has been estimated to be 5 to 11 mmol per g

Received 20 May 2015 Accepted 12 September 2015

Accepted manuscript posted online 18 September 2015

Citation Henningsen BM, Hon S, Covalla SF, Sonu C, Argyros DA, Barrett TF, Wiswall E, Froehlich AC, Zelle RM. 2015. Increasing anaerobic acetate consumption and ethanol yields in *Saccharomyces cerevisiae* with NADPH-specific alcohol dehydrogenase. *Appl Environ Microbiol* 81:8108–8117. doi:10.1128/AEM.01689-15.

Editor: A. A. Brakhage

Address correspondence to Rintze M. Zelle, rzelle@allemand.com.

* Present address: Shuen Hon, Thayer School of Engineering, Dartmouth College, Hanover, New Hampshire, USA.

Supplemental material for this article may be found at <http://dx.doi.org/10.1128/AEM.01689-15>.

Copyright © 2015, American Society for Microbiology. All Rights Reserved.

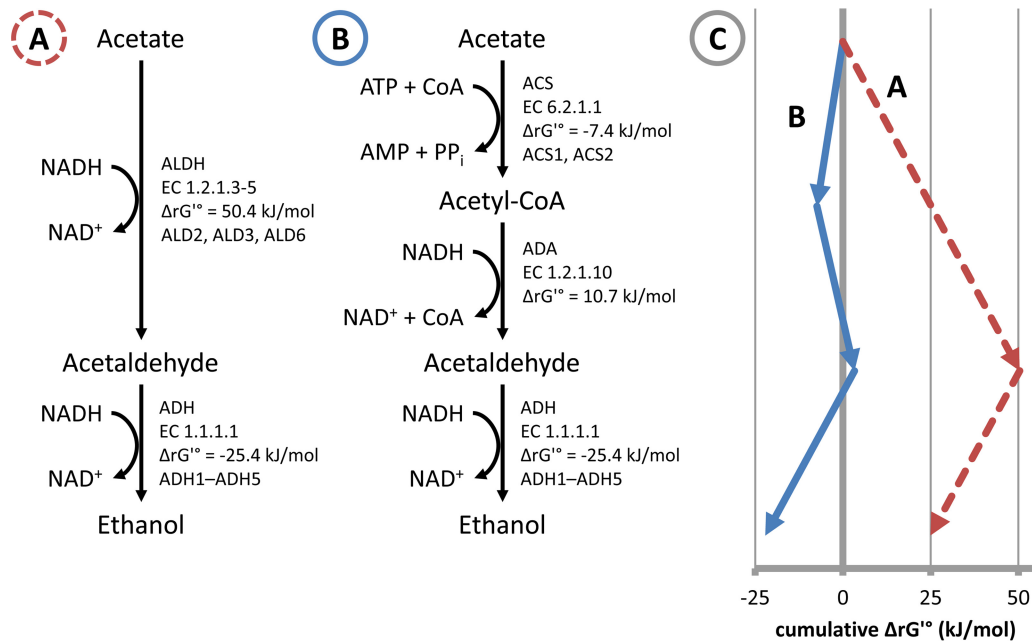


FIG 1 (A, B) Endogenous ALDH/ADH (A) and engineered ACS/ADA/ADH (B) pathways for the conversion of acetate to ethanol in *S. cerevisiae*. For simplicity, all redox reactions are presented with NADH as the cofactor. Reactions list their associated endogenous genes. ΔrG° values, indicating each reaction's Gibbs free energy change in the forward direction at pH-neutral standard state conditions, were obtained from the eQuilibrator website (49). (C) Cumulative ΔrG° values illustrate that the ACS/ADA/ADH pathway (pathway B) is thermodynamically favorable, unlike the ALDH/ADH pathway (pathway A). Abbreviations: ACS, AMP-forming acetyl-CoA synthetase; ADA, acetaldehyde dehydrogenase (acetylating); ADH, alcohol dehydrogenase; ALDH, nonacetylating acetaldehyde dehydrogenase.

cells (dry weight) (CDW) produced (18, 21, 22), limiting the amount of acetate that can be consumed by glycerol-3-phosphate dehydrogenase-negative (Gpd^-) ADA-expressing *S. cerevisiae* strains. Guadalupe Medina et al. reported consumption of 0.022 and 0.012 g acetate (g glucose)⁻¹ for a nonevolved and an evolved Gpd^- ADA strain, respectively (18, 23). Based on the metabolite profile of the parental wild-type strain, the authors calculated a surplus of 7.8 mmol NADH per g CDW produced, which was reoxidized via the consumption of 3.9 mmol (0.23 g) acetate per g CDW. This is close to the consumption of 0.27 g acetate per g CDW produced that was observed for their nonevolved Gpd^- ADA strain (18).

To circumvent this redox constraint, Wei et al. elegantly combined the ACS/ADA/ADH pathway with xylose fermentation via xylose reductase (XR) and xylitol dehydrogenase (XDH) (24). Introducing NAD(P)H-specific XR and NADH-specific XDH from *Scheffersomyces stipitidis* into *S. cerevisiae* is known to confer the ability to ferment xylose (25), but the differing redox cofactor preferences of these enzymes result in increased NADPH demand and overproduction of NADH during growth on xylose. This redox imbalance is especially problematic during anaerobic fermentation and has led to efforts to either match the cofactor preference of XR and XDH (26) or to use the cofactor-independent xylose isomerase instead (9, 27). Wei et al. used this redox imbalance to their advantage by redirecting the surplus NADH of xylose consumption to the conversion of acetate to ethanol, showing consumption of 0.031 g acetate (g xylose)⁻¹ in a Gpd^+ background (24). No genetic changes were required to satisfy the increased NADPH demand, consistent with findings that the oxidative pentose phosphate pathway flexibly responds to increased NADPH consumption (22).

An alternative approach to generate additional cytosolic NADH for acetate uptake is the conversion of glycerol to ethanol, which can yield one NADH per glycerol consumed. This strategy has been pursued by overexpression of NADH-specific glycerol dehydrogenase and dihydroxyacetone kinase (28; J. A. M. de Bont, A. W. R. H. Teunissen, P. Klaassen, W. W. A. Hartman, and S. van Beusekom, June 2013, world patent WO2013081456). In a fed-batch system with corn fiber hydrolysate, an impressive 0.10 g acetate (g sugar)⁻¹ was converted by Gpd^+ strains, with a total consumption of 7.5 g liter⁻¹ acetate and 18 g liter⁻¹ glycerol (de Bont et al., world patent WO2013081456).

In this study, we present a novel strategy to generate additional cytosolic NADH in *S. cerevisiae* during anaerobic ethanolic fermentation, based on tuning of the cofactor preference of cytosolic alcohol dehydrogenase. This allows more acetate to be converted to ethanol, further decreasing acetate toxicity and improving ethanol yields. In contrast to the xylose- and glycerol-based strategies described above, our approach is not dependent on the availability of specific sugars or cosubstrates besides acetate.

MATERIALS AND METHODS

Strains and strain maintenance. All strains in this study (Table 1) are derived from M2390, a diploid *S. cerevisiae* strain used in the bioethanol industry. Strains were stored in yeast extract-peptone-dextrose (YPD) medium with 15% (wt/vol) glycerol at -80°C and struck to YPD plates before use. The YPD medium consisted of 10 g liter⁻¹ yeast extract (210941; BD Difco), 20 g liter⁻¹ bacteriological peptone (20048; Afymetrix USB), and, unless noted otherwise, 20 g liter⁻¹ glucose (Cerelease dextrose monohydrate 020010; Ingredion).

The genomic modifications were performed with integration cassettes, consisting of purified overlapping PCR products, essentially as described previously (A. Argyros, W. R. Sillers, T. Barrett, N. Caiazza, and

TABLE 1 Strains used in this study^a

Strain	Genotype
M2390	<i>MATa/MATα</i> (wild-type, industrial diploid <i>S. cerevisiae</i> strain)
M6571	<i>MATa/MATα gpd1Δ::Ba-adhE gpd2Δ::Ba-adhE</i>
M6951	<i>MATa/MATα gpd1Δ::Ba-adhE gpd2Δ::Ba-adhE fcy1Δ::Eh-ADH1</i>
M7888	<i>MATa/MATα gpd1Δ::Ba-adhE gpd2Δ::Ba-adhE fcy1Δ::Eh-ADH1 ylr296wΔ::pADH1-ZWF1</i>
M7890	<i>MATa/MATα gpd1Δ::Ba-adhE gpd2Δ::Ba-adhE fcy1Δ::Eh-ADH1 ylr296wΔ::ACS2</i>
M8031	<i>MATa/MATα gpd1Δ::Ba-adhE gpd2Δ::Ba-adhE fcy1Δ::Eh-ADH1 ylr296wΔ::[ACS2 pADH1-ZWF1]</i>
M9188	<i>MATa/MATα gpd1Δ::Ba-adhE gpd2Δ::Ba-adhE ylr296wΔ::pADH1-ZWF1</i>
M9190	<i>MATa/MATα gpd1Δ::Ba-adhE gpd2Δ::Ba-adhE ylr296wΔ::ACS2</i>
M9192	<i>MATa/MATα gpd1Δ::Ba-adhE gpd2Δ::Ba-adhE ylr296wΔ::[ACS2 pADH1-ZWF1]</i>
M9843	<i>MATa/MATα gpd1Δ::Ba-adhE gpd2Δ::Ba-adhE fcy1Δ::Eh-ADH1 ylr296wΔ::ACS2 apt2Δ::pHXT2-ZWF1</i>

^a All modifications are homozygous. With the exception of *ZWF1*, promoters and terminators used to express introduced genes have been omitted. Square brackets indicate integration of multiple genes at a single locus. *Ba-adhE*, *B. adolescentis adhE* (GenBank accession no. [BAF39100.1](#)); *Eh-ADH1*, *E. histolytica ADH1* (GenBank accession no. [M88600.1](#)).

A. J. Shaw, October 2012, world patent WO2012138942). After transformation of the PCR fragments into *S. cerevisiae*, homologous recombination allowed the cassettes to be assembled *in vivo* and integrated. To encourage integration at the desired chromosomal site, the outer sequences of each cassette matched the regions flanking the genomic target site. Integration sites were first marked with cassettes containing selectable and counterselectable markers, replacing the targeted open reading frame. The marker cassettes were subsequently replaced with the desired DNA sequence in a second transformation using counterselection. To ensure simultaneous integration at both alleles, two variants of each marker cassette were used with different selection markers (e.g., for G418 and hygromycin resistance). Integrations were confirmed by PCR.

Transformations. For *S. cerevisiae* transformations, the strains were grown overnight in 5 ml YPD in 14-ml round-bottom tubes at 35°C in a roller drum. The cells were harvested by centrifugation, washed once in 5 ml H₂O, and resuspended in 0.8 ml of 100 mM lithium acetate in 1× Tris-EDTA (TE) buffer. After addition of 20 μl of 1 M dithiothreitol (DTT), the cell suspension was incubated for 30 min at 35°C. The cells were centrifuged, washed twice in 1 ml H₂O, resuspended in 200 μl of 1 M sorbitol, and kept on ice. Then 100-μl aliquots of the cell suspension were added to precooled 2-mm-gap electroporation cuvettes and mixed with up to 20 μl DNA solution. For the homologous recombination-based genomic integrations, approximately 0.15 pmol (100 ng kb⁻¹) of each PCR product was used. Following 2.5-kV electroporation in a Bio-Rad Gene Pulser Xcell electroporator, the cell suspension was combined with 1 ml YPD with 0.5 M sorbitol, and cells were allowed to recover at 35°C in the roller drum before being plated to the appropriate selective agar medium.

Serum bottle fermentations. The strains were grown overnight in 5 ml YPD in 14-ml round-bottom tubes at 35°C in a roller drum. The precultures were harvested by centrifugation, washed in 2 ml H₂O, and resuspended in 2 ml H₂O. Then 100-μl cell suspensions were used to inoculate 20 ml medium in 120-ml serum bottles. The bottles were sealed with rubber stoppers. For flushed bottles, the headspace was evacuated with a vacuum pump and replaced with a mixture of 95% N₂ and 5% CO₂ in 4 evacuation/fill cycles. To prevent excessive pressure buildup, the stoppers in the bottles with >40 g liter⁻¹ glucose were pierced with a needle. The bottles were incubated at 35°C in an orbital shaker at 175 rpm.

The defined medium consisted of glucose, 5 g liter⁻¹ (NH₄)₂SO₄, 3 g liter⁻¹ KH₂PO₄, 0.5 g liter⁻¹ MgSO₄ · 7 H₂O, vitamins (set to pH 6.5) and trace elements (29), Tween 80 (0.42 g liter⁻¹), and ethanol-dissolved ergosterol (10 mg liter⁻¹). Acetate was added to the medium as potassium acetate (P1190; Sigma), and pH adjustments were made with HCl. All medium components were filter sterilized.

Biomass analysis. Optical densities were determined at 600 nm using a Molecular Devices SpectraMax M2 spectrophotometer. The cell weight (dry weight) was determined by centrifuging 10 ml broth, washing with H₂O, and drying the pellet overnight at 105°C in a preweighed container.

Carbon balances. To determine carbon recoveries (calculated as millimoles of carbon), concentrations of lactate, glycerol, acetate, ethanol, and glucose were measured by high-performance liquid chromatography (HPLC) for the medium and the end-of-fermentation samples. The carbon content of dry biomass was assumed to be 48% (wt/wt). CO₂ production was calculated based on the weight loss of the vented serum bottles.

Metabolite analysis. The extracellular concentrations of acetate, ethanol, glucose, glycerol, and lactate in the culture supernatant were determined with an Agilent 1200 series HPLC, using a Bio-Rad Aminex HPX-87H ion-exchange column eluted with 5 mM H₂SO₄ at a flow rate of 0.7 ml min⁻¹ at 65°C. All metabolites were detected with an Agilent 1200 series refractive index detector. To prepare for HPLC measurement, supernatant samples were acidified with 20 μl of 10% H₂SO₄ per 400 μl supernatant and run through a 0.2-μm microspin filter. Ethanol concentrations are reported as measured, but ethanol yields have been corrected for the ethanol present in the defined medium.

Preparation of cell-free extracts for *in vitro* enzyme assays. The strains were grown overnight in 5 ml YPD at 35°C in a roller drum. In an oxygen-free chamber, 500-ml baffled shake flasks were filled with 200 ml YPD (40 g liter⁻¹ glucose, 5 g liter⁻¹ acetate), inoculated with the overnight cultures, and equipped with one-way venting valves. After 24 h of incubation at 35°C and 120 rpm, cells were spun down at 4°C (5 min at 5,000 rpm), washed in H₂O, and resuspended in H₂O before aliquoting and storage at -80°C. To prepare the cell extracts, frozen samples were thawed and centrifuged to remove the supernatant. For the ACS and glucose-6-phosphate dehydrogenase (G6PDH) assays, a 0.5-g cell pellet was lysed by the addition of 1 ml Y-PER Plus reagent (78999; Thermo Scientific) in the presence of 100 mM DTT and a 1:1,000 dilution of protease inhibitor cocktail (P8215; Sigma). After a 20-min incubation at 4°C, the lysate was centrifuged for 5 min at 15,000 × g, after which the supernatant was saved on ice for subsequent analysis. For the ADH assay, up to half a gram (0.5 g) of cell pellet was washed and resuspended in 1 ml of 100 mM potassium phosphate buffer (pH 7.5) containing 2 mM MgCl₂ and 1 mM DTT. The cells were subsequently disrupted in a FastPrep homogenizer (MP Biomedicals) in the presence of 0.75 g glass beads (0.5-mm diameter) (11079105; BioSpec), in 4 bursts of 20 s with 1-min cooldowns on ice in between. The lysate was centrifuged for 20 min at 15,000 rpm at 4°C, after which the supernatant was saved on ice for subsequent analysis. Protein concentrations were determined with the Bio-Rad protein assay (500-0006; Bio-Rad) using bovine serum albumin (BSA) as the standard.

***In vitro* enzyme assays.** (i) ACS. The *in vitro* ACS assay was based on the acetic acid (ACS manual format) kit (K-ACET; Megazyme), which relies on citrate synthase and L-malate dehydrogenase to link the acetyl-CoA formation to NAD⁺ reduction, and performed as previously described (30). Cell extract replaced the sample, and the reactions were started with 10 mM potassium acetate instead of ACS. Enzyme activities were determined by observing NAD⁺ reduction at 340 nm and 37°C.

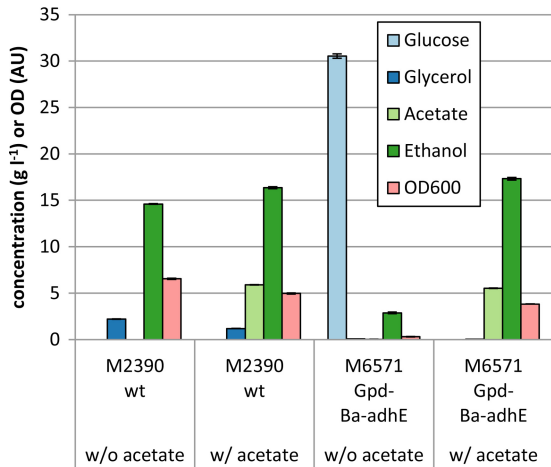


FIG 2 Metabolite profiles of *S. cerevisiae* strains M2390 and M6571 cultivated in flushed (95% N₂-5% CO₂) sealed serum bottles with defined medium (35 ± 0.2 g liter⁻¹ glucose with or without 6.0 g liter⁻¹ acetate [pH 5.5]), sampled after 70 h. The medium contained 1.0 ± 0.1 g liter⁻¹ ethanol due to ergosterol addition. Bottles were run in triplicate, and error bars show standard deviations. Genotypes: wt, wild type; Gpd⁻, *gpd1Δ gpd2Δ* deletion; Ba-adhE, *B. adolescentis adhE* expression. OD600, optical density at 600 nm; AU, arbitrary units.

(ii) **ADH.** The ADH assay was based on the method of Kumar et al. (31). The assay mixture consisted of 50 mM glycine-NaOH buffer (pH 9.5) and 1 mM NADP⁺. The reaction was started with 100 mM ethanol. Enzyme activities were determined by observing NADP⁺ reduction at 340 nm and 35°C.

(iii) **G6PDH.** The G6PDH assay mixture contained 50 mM Tris-HCl (pH 7.8), 5 mM MgCl₂, and 0.6 mM NADP⁺ (30). The reaction was

started with 5 mM glucose-6-phosphate. Enzyme activities were determined by observing NADP⁺ reduction at 340 nm and 37°C.

RESULTS

Construction of a Gpd⁻ ADA *S. cerevisiae* strain. To eliminate glycerol formation and to complete the ACS/ADA/ADH pathway for the conversion of acetate to ethanol, the glycerol-3-phosphate dehydrogenase genes *GPD1* and *GPD2* were deleted in M2390, a diploid wild-type *S. cerevisiae* strain used in the bioethanol industry, and replaced with expression cassettes for the bifunctional ADA/ADH-encoding *adhE* gene from *Bifidobacterium adolescentis* (Ba-*adhE*), resulting in strain M6571.

When strain M2390 was grown on defined medium with 35 g liter⁻¹ glucose in oxygen-free bottles (flushed with a mixture of 95% nitrogen and 5% carbon dioxide), the addition of 6.0 g liter⁻¹ acetate reduced the production of biomass and glycerol and increased the ethanol titer, reflecting the toxicity of acetate (Fig. 2). In contrast, the Gpd⁻ Ba-*adhE* M6571 strain, in which the main pathway for glycerol production was interrupted, failed to grow unless acetate was added as an external electron acceptor. With acetate, M6571 reached higher ethanol titers than M2390, primarily the result of abolished glycerol production and increased acetate consumption.

Strain M6571 was subsequently compared to strain M2390 at glucose and acetate concentrations more representative of industrial cellulosic hydrolysates. In unflushed YPD bottle fermentations with 117 g liter⁻¹ glucose and 8.3 g liter⁻¹ acetate, M6571 showed strongly reduced glycerol production (final titers of 2.6 ± 0.0 and 0.1 ± 0.0 g liter⁻¹ for M2390 and M6571, respectively). Acetate consumption increased from 0.6 to 1.3 g liter⁻¹ (final titers of 7.7 ± 0.0 and 7.0 ± 0.3 g liter⁻¹), and the ethanol titer increased from 51.6 ± 0.1 to 54.1 ± 0.3 g liter⁻¹ (Fig. 3). Based on

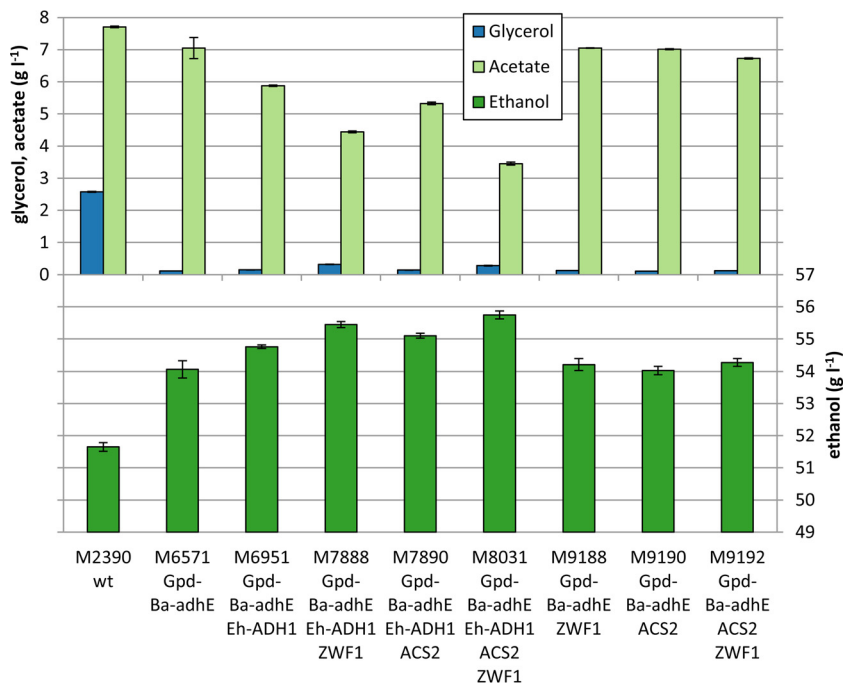


FIG 3 Metabolite profiles of *S. cerevisiae* strains cultivated in unflushed vented serum bottles with YPD (117 g liter⁻¹ glucose, 8.3 g liter⁻¹ acetate [pH 5.5]), sampled after 75 h. Bottles were run in triplicate, and error bars show standard deviations. Genotypes: wt, wild type; Gpd⁻, *gpd1Δ gpd2Δ* deletion; Ba-adhE, *B. adolescentis adhE* expression; Eh-ADH1, *E. histolytica ADH1* expression; ZWF1, *ZWF1* overexpression with the *ADH1* promoter; ACS2, *ACS2* overexpression.

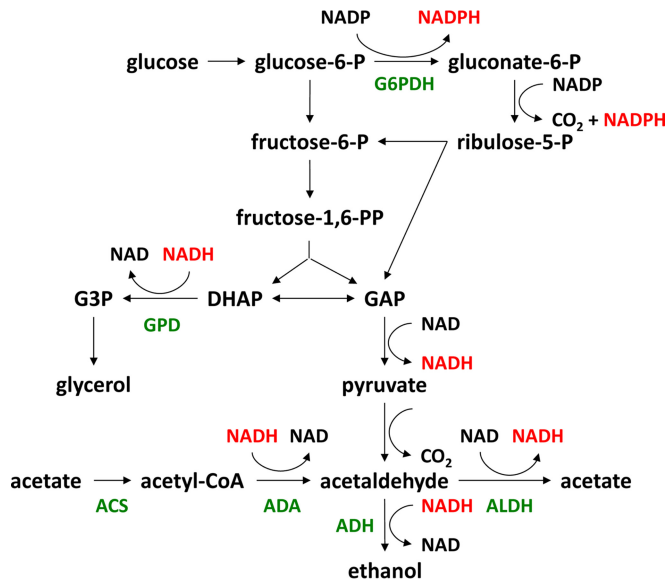


FIG 4 Main redox pathways of interest in *S. cerevisiae* during anaerobic growth on glucose. Glycolysis allows for the redox-neutral conversion of glucose to ethanol and CO₂. Redirecting glucose-6-phosphate (glucose-6-P) into the oxidative pentose phosphate pathway generates net NADPH and additional CO₂ at the expense of ethanol, whereas converting glucose to glycerol consumes NADH. Converting acetate to ethanol in strains expressing heterologous NADH-specific ADA consumes NADH. Abbreviations: ACS, acetyl-CoA synthetase; ADA, acetaldehyde dehydrogenase (acetylating); ADH, alcohol dehydrogenase; ALDH, nonacetylating acetaldehyde dehydrogenase; GPD, glycerol-3-phosphate dehydrogenase; G6PDH, glucose-6-phosphate dehydrogenase; DHAP, dihydroxyacetone phosphate; G3P, glycerol-3-phosphate; GAP, glyceraldehyde 3-phosphate.

the redox stoichiometry of displacing glycerol formation with the conversion of acetate to ethanol (for calculations, see File S1 in the supplemental material), a 2.5-g liter⁻¹ lower glycerol titer should result in an NADH surplus of 27 mM, allowing for consumption of 0.8 g liter⁻¹ acetate and production of an additional 1.8 g liter⁻¹ ethanol (the extra ethanol comes both from acetate and from glucose that is no longer converted to glycerol). The reasonably close agreement between the theoretical and experimental numbers matched our previous findings in Gpd⁻ ADA strains (W. R. Sillers, H. van Dijken, S. Licht, A. J. Shaw, A. B. Gilbert, A. Argyros, A. C. Froehlich, J. E. McBride, H. Xu, D. A. Hogsett, and V. B. Rajgarhia, November 2011, world patent WO2011140386) and supported our assumption that *B. adolescentis* adhEp is predominantly NADH specific, while suggesting that NADH availability in strain M6571 is likely a limiting factor in the conversion of acetate to ethanol.

Expression of *Entamoeba histolytica* ADH1. The main metabolic pathways for glucose fermentation in *S. cerevisiae* are shown in Fig. 4. By deletion of the GPD genes and expression of ADA in strain M6571, the surplus NADH generated in the production of biomass was successfully redirected from glycerol production to conversion of acetate to ethanol via ACS/ADA/ADH. However, wild-type *S. cerevisiae* strains have limited flexibility to generate additional NADH during anoxic conditions without incurring a great loss in ethanol yield and initiating undesirable by-product formation. For example, excretion of one pyruvate generates one NADH but costs one ethanol. Production of acetate from acetaldehyde via NADH-specific aldehyde dehydrogenase generates

two NADH per ethanol sacrificed, but this directly counters the desired conversion of extracellular acetate into ethanol.

Interestingly, anaerobic NADPH production in *S. cerevisiae* is more flexible and can be more carbon efficient. The oxidative pentose phosphate pathway (oxPPP) plays a crucial role in wild-type *S. cerevisiae* strains in satisfying the biosynthetic NADPH requirement (21, 32, 33) and can easily adapt to increased NADPH demand (22). Whereas ethanolic fermentation via glycolysis produces equimolar amounts of ethanol and CO₂, the oxPPP shifts this ratio toward CO₂ production. The large difference in the degree of reduction between ethanol and CO₂ results in a high electron yield of 6 NADPH per ethanol sacrificed (for calculations, see File S1 in the supplemental material).

The cytosolic ADH activity is predominantly NADH specific during ethanolic fermentation in wild-type *S. cerevisiae* (19). We hypothesized that introducing a cytosolic NADPH-specific alcohol dehydrogenase (NADPH-ADH) would increase the cell's metabolic flexibility and allow for redox balancing between the NADPH produced in the oxPPP and the NADH consumed in the conversion of acetate to ethanol (Fig. 5). Stoichiometric calculations show that such an approach allows the conversion of up to 0.29 g acetate per g glucose. At this theoretical maximum, all ATP generated in the fermentation of glucose would be dedicated to converting acetate to ethanol, leaving no room for cellular growth and maintenance, while two-thirds of all ADH activity would be NADPH dependent (see File S1 in the supplemental material).

To test this hypothesis, we expressed *ADH1* from the protozoan parasite *Entamoeba histolytica* (Eh-*ADH1*), encoding an NADPH-specific alcohol dehydrogenase with high activity and affinity toward acetaldehyde (31), in strain M6571 to produce strain M6951. The expression was confirmed with an *in vitro* enzyme assay, which showed a 10-fold increase in NADPH-ADH activity in M6951 compared to that in M6571 (Table 2). Expression of Eh-*ADH1* increased acetate consumption by 1.2 g liter⁻¹ (final titer of 5.9 ± 0.0 g liter⁻¹) and ethanol production by 0.7 g liter⁻¹ (final titer of 54.8 ± 0.1 g liter⁻¹) in the YPD bottle fermentations (Fig. 3). These titer changes were in agreement with an oxPPP redox-balanced yield of 0.51 g ethanol per g acetate (for calculations, see File S1 in the supplemental material).

Overexpression of ACS2 and ZWF1. The Gpd⁻ Ba-*adhE* Eh-*ADH1* strain M6951 consumed 0.021 g acetate per g glucose (Fig. 3). Since this was still significantly below the theoretical maximum of 0.29 g g⁻¹, we explored additional genetic modifications.

We first focused on *ZWF1*, encoding glucose-6-phosphate dehydrogenase (G6PDH) (34), which catalyzes the first reaction of the oxidative pentose phosphate pathway (Fig. 4). *ZWF1* has been linked to furfural and H₂O₂ tolerance (10, 35, 36), presumably by providing NADPH for detoxification reactions, and has been overexpressed to generate NADPH for xylitol production (37, 38).

Overexpression of *ZWF1* in strain M6951 resulted in strain M7888. Compared to that by M6951, acetate consumption by M7888 (Gpd⁻ Ba-*adhE* Eh-*ADH1* *ZWF1*) increased by 1.4 g liter⁻¹ (final titer of 4.4 ± 0.0 g liter⁻¹) (Fig. 3), while the ethanol titer increased by 0.7 g liter⁻¹ (final titer of 55.4 ± 0.1 g liter⁻¹). The final glycerol titer increased slightly from 0.1 ± 0.0 to 0.3 ± 0.0 g liter⁻¹. A similar increase in glycerol production was observed by Guadalupe Medina et al. after evolution of a Gpd⁻ ADA strain, which was speculated to be due to increased glycerolipid degradation (23, 39).

We also targeted acetyl-CoA synthetase (ACS), which converts

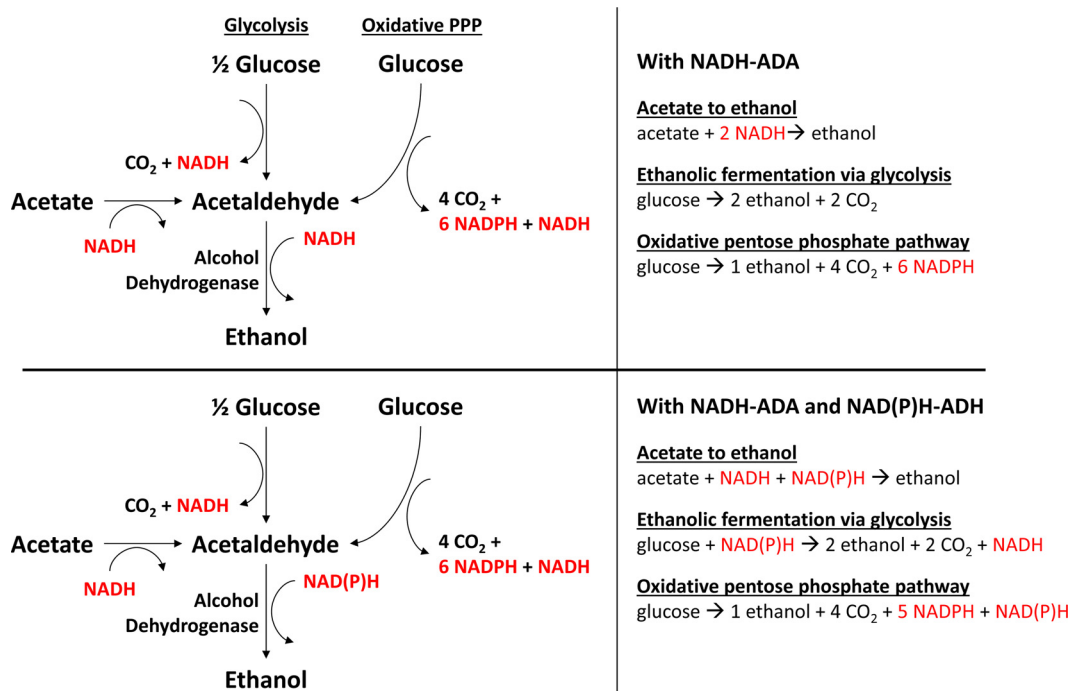


FIG 5 Redox pathways in a Gpd^- *S. cerevisiae* strain expressing NADH-specific acetaldehyde dehydrogenase (acetylating) (ADA) in the absence (top) or presence (bottom) of cytosolic NADPH-specific alcohol dehydrogenase (ADH). The combined presence of NADH- and NADPH-specific ADH allows the redox cofactors of the oxidative pentose phosphate pathway and the acetate-to-ethanol pathway to be matched, with ethanolic fermentation via glycolysis playing a crucial role in exchanging NADPH for NADH.

acetate to acetyl-CoA in the first reaction of the acetate-to-ethanol pathway. ACS has been a target in multiple metabolic engineering strategies with *S. cerevisiae* for overproduction of acetyl-CoA-derived products (40–42), as well as for overproduction of NADPH for aerobic xylitol production (43). We chose to overexpress ACS2, which unlike ACS1 is not subject to glucose catabolite inactivation (44).

Overexpression of ACS2 in strain M6951 resulted in strain M7890. Compared to that by M6951, acetate consumption by M7890 (Gpd^- Ba-*adhE* Eh-*ADH1* ACS2) increased by 0.6 g liter⁻¹ (final titer of 5.3 ± 0.0 g liter⁻¹), while the ethanol titer increased by 0.3 g liter⁻¹ (final titer of 55.1 ± 0.1 g liter⁻¹) (Fig. 3).

Combining the overexpression of ACS2 and *ZWF1* in strain M6951 had a synergistic effect in the resulting strain M8031 (Gpd^- Ba-*adhE* Eh-*ADH1* ACS2 *ZWF1*). Acetate consumption

increased by 2.4 g liter⁻¹ (final titer of 3.5 ± 0.0 g liter⁻¹), and ethanol production increased by 1.0 g liter⁻¹ (final titer of 55.7 ± 0.1 g liter⁻¹) (Fig. 3). Similar to M7888, M8031 showed a slightly increased glycerol titer of 0.3 ± 0.0 g liter⁻¹. If we assume that the oxPPP provides the electrons needed to convert acetate to ethanol, the extra 3.6 g liter⁻¹ acetate consumed by M8031 compared to M6571 can be expected to allow the production of 1.8 g liter⁻¹ ethanol, closely matching the experimental results. Compared to the wild-type M2390 reference strain, M8031 showed an 8% higher ethanol yield on glucose (0.48 ± 0.0 g g⁻¹ versus 0.44 ± 0.0 g g⁻¹), while acetate consumption increased from 0.005 ± 0.000 to 0.041 ± 0.000 g acetate per g glucose.

In vitro enzyme assays showed that overexpression of ACS2 in strains M7890 and M8031 increased ACS activity by approximately 4-fold, whereas overexpression of *ZWF1* in strains

TABLE 2 *In vitro* enzyme activities of NADPH-specific alcohol dehydrogenase, acetyl-CoA synthetase, and glucose-6-phosphate dehydrogenase

Strain	Description ^a	Enzyme activity (μmol min ⁻¹ mg protein ⁻¹) ^b		
		NADPH-ADH	ACS	G6PDH
M2390	Wild type	0.002 ± 0.000	0.03 ± 0.00	0.18 ± 0.08
M6571	Gpd^- Ba- <i>adhE</i>	0.003 ± 0.000	0.04 ± 0.00	0.17 ± 0.02
M6951	Gpd^- Ba- <i>adhE</i> Eh- <i>ADH1</i>	0.031 ± 0.003	0.04 ± 0.00	0.17 ± 0.03
M7888	Gpd^- Ba- <i>adhE</i> Eh- <i>ADH1</i> p <i>ADH1-ZWF1</i>	ND ^c	0.03 ± 0.00	5.46 ± 0.14
M7890	Gpd^- Ba- <i>adhE</i> Eh- <i>ADH1</i> ACS2	ND	0.17 ± 0.05	0.23 ± 0.04
M8031	Gpd^- Ba- <i>adhE</i> Eh- <i>ADH1</i> ACS2 p <i>ADH1-ZWF1</i>	ND	0.11 ± 0.03	4.49 ± 0.52
M9843	Gpd^- Ba- <i>adhE</i> Eh- <i>ADH1</i> ACS2 p <i>HXT2-ZWF1</i>	0.033 ± 0.002	0.13 ± 0.02	0.71 ± 0.05

^a Gpd^- , *GPD1/GPD2* deletion; Ba-*adhE*, *B. adolescentis adhE* acetaldehyde dehydrogenase (acetylating), Eh-*ADH1*, *E. histolytica ADH1*.

^b Values represent the average ± SD for duplicate cultures. NADPH-ADH, NADPH-specific alcohol dehydrogenase; ACS, acetyl-CoA synthetase; G6PDH, glucose-6-phosphate dehydrogenase.

^c ND, not determined.

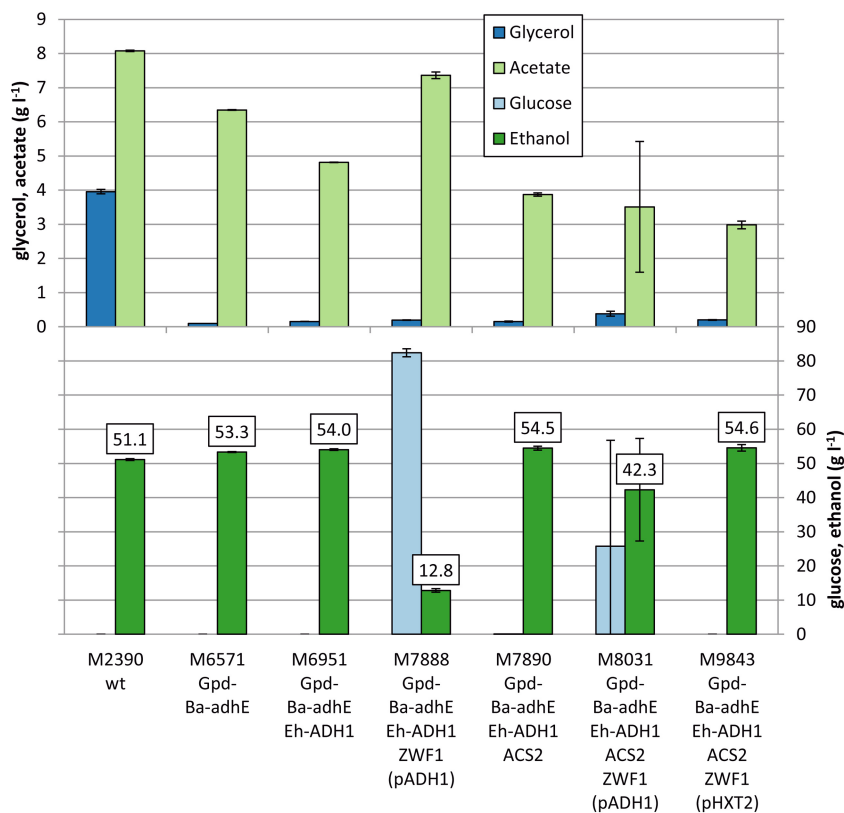


FIG 6 Metabolite profiles of *S. cerevisiae* strains cultivated in flushed (95% N₂-5% CO₂) vented serum bottles with defined medium (114 g liter⁻¹ glucose, 8.3 g liter⁻¹ acetate, pH 5.5), sampled after 120 h. The medium contained 0.7 g liter⁻¹ ethanol due to ergosterol addition. Bottles were run in triplicate, and error bars show standard deviations. Genotypes: wt, wild type; Gpd⁻, *gpd1Δ gpd2Δ* deletion; Ba-*adhE*, *B. adolescentis adhE* expression; Eh-ADH1, *E. histolytica ADH1* expression; ZWF1, *ZWF1* overexpression with either the *ADH1* or *HXT2* promoter; ACS2, *ACS2* overexpression.

M7888 and M8031 increased G6PDH activity by ca. 26-fold (Table 2).

Role of Eh-ADH1 in strains overexpressing ACS2 and ZWF1.

To confirm that Eh-ADH1 played its envisaged role as redox balancer, we deleted the gene in strains M7888, M7890, and M8031, resulting in strains M9188, M9190, and M9192, respectively. All three strains performed similarly to strain M6571 (Fig. 3) with limited acetate consumption. This supports our assumption that conversion of acetate to ethanol in M6571 is indeed primarily NADH limited, since *ACS2* overexpression loses its effectiveness in strains lacking Eh-ADH1 (M9190 and M9192). It also provides additional evidence that NADPH-specific Eh-ADH1 can successfully compete with endogenous cytosolic NADH-specific ADH and allows NADPH generated in the oxPPP to be exchanged for NADH for use by the NADH-specific ADA, since *ZWF1* overexpression no longer benefits acetate consumption in strains lacking Eh-ADH1 (M9188 and M9192).

Fine-tuning ZWF1 expression for anaerobic performance.

Whereas strains M7888 and M8031 performed well in unflushed bottles with YPD medium (Fig. 3), we found that both *ZWF1*-overexpressing strains grew poorly in bottles flushed with 95% N₂-5% CO₂, especially in defined medium, resulting in high residual glucose and poor ethanol yields (Fig. 6). Whereas all bottles with M7888 seemed to have stalled at ca. 80 g liter⁻¹ glucose after 120 h, residual glucose for M8031 ranged from 2 to 61 g liter⁻¹ among the replicates. With a gas-to-liquid ratio of 5:1, unflushed

bottles had an effective oxygen dose of ca. 43 mM. This might allow for the respiration of ca. 1 g liter⁻¹ glucose and might provide the *ZWF1*-overexpressing yeast strains the time and energy to adapt to the anaerobic redox constraints. Alternatively, the oxygen might simply allow for sufficient initial growth to allow the fermentation to finish, even if growth slows once anoxic conditions have been achieved.

In view of the very high G6PDH enzyme activity levels measured for the *ZWF1*-overexpressing strains M7888 and M8031, we hypothesized that these strains might suffer from too much G6PDH activity under anoxic conditions. Since robust anaerobic performance is crucial for industrial application, we tried overexpressing *ZWF1* in M7890 with a different promoter (*pHXT2* instead of *pADH1*), resulting in strain M9843 (Gpd⁻ Ba-*adhE* Eh-ADH1 ACS2 *pHXT2*-*ZWF1*). This moderated the *ZWF1* activity to 0.71 ± 0.05 μmol min⁻¹ (mg protein)⁻¹, ca. 4-fold over the wild-type level (Table 2), and greatly improved growth in flushed bottles (Fig. 6).

The engineered strains that were able to finish in flushed bottles with defined medium generally showed better acetate uptake than those in unflushed YPD bottles (Fig. 6). Compared to that in M2390, glycerol production was again greatly reduced in the Gpd⁻ Ba-*adhE* M6571 strain, with final titers of 4.0 ± 0.1 and 0.1 ± 0.0 g liter⁻¹, respectively. Acetate uptake increased from 0.2 to 1.9 g liter⁻¹ (with final titers of 8.1 ± 0.0 g liter⁻¹ for M2390 and 6.3 ± 0.0 g liter⁻¹ for M6571), and ethanol production increased

by 4% (final titers of 51.1 ± 0.3 and 53.3 ± 0.1 g liter⁻¹). Additional overexpression of *Eh-ADH1*, *ACS2*, and *ZWF1* (the latter under the control of *pHXT2*) in strain M9843 raised acetate consumption by a further 3.4 g liter⁻¹ (final titer of 3.0 ± 0.1 g liter⁻¹) while increasing ethanol production by 1.2 g liter⁻¹ (final titer of 54.6 ± 1.0 g liter⁻¹), somewhat less than the 1.7 g liter⁻¹ extra ethanol expected based on the difference in acetate uptake, which can partially be explained by a slight increase in glycerol production to 0.2 g liter⁻¹. M9843 consumed 0.046 ± 0.001 g acetate per g glucose and showed a 7% higher ethanol yield on glucose than the wild-type reference strain M2390 (0.47 ± 0.01 g g⁻¹ versus 0.44 ± 0.00 g g⁻¹).

DISCUSSION

NADPH-ADH as a target for redox engineering. To our knowledge, this study is the first to report the use of NADPH-specific alcohol dehydrogenase in *S. cerevisiae* for the net production of NADH during anaerobic ethanolic fermentation. Unlike previous efforts to increase acetate consumption during ethanol fermentation by supplying additional NADH (24, 28; de Bont et al., world patent WO2013081456), the use of NADPH-ADH does not require specific sugar substrates such as xylose or cosubstrates such as glycerol. Our approach creates a tunable redox imbalance in ethanolic fermentation, where NADH generated in glycolysis is partially preserved and the increased demand for NADPH is fulfilled by the oxidative pentose phosphate pathway. Celton et al. used a stoichiometric model to estimate that the native pentose phosphate pathway can generate as much as 140 mmol NADPH per g CDW (22), significantly more than the anaerobic NADH surplus of 5 to 11 mmol per g CDW (18, 21, 22). As such, NADPH-ADH might be of use to other metabolic engineering projects in yeast that involve electron-consuming side reactions of ethanolic fermentation for which only NADH-consuming enzymes are available. The applicability of NADPH-ADH in metabolic engineering strategies was recently underlined by an *in silico* analysis of cofactor swaps in a genome-scale metabolic model of *S. cerevisiae*, where ADH was identified as a powerful target for overproducing native metabolites (45).

Industrial acetate consumption strains. The acetate consumption strains described in this study have glycerol-3-phosphate dehydrogenase genes *GPD1* and *GPD2* deleted. While a convenient genetic modification to avoid competition for the anaerobic biosynthetic NADH surplus, *Gpd*⁻ strains are known to be sensitive to osmotic stress and to be less robust (23, 46). However, a reduction in glycerol formation is still very much desired since it increases the ethanol yield. Therefore, to create industrially applicable acetate consumption strains via the metabolic engineering strategy presented, a future objective is to (partially) re-enable glycerol formation while maintaining a careful balance between glycerol formation and acetate consumption, either through single deletions of the GPD genes or downregulation of their expression (47, 48).

In this light, it is interesting that while the ACS/ADA/ADH pathway was first demonstrated in a *gpd1Δ gpd2Δ* background (18), it has since been implemented in *GPD1 GPD2* strains (24, 28), with Wei et al. reporting that glycerol production was kept in check by selecting a better ADA enzyme. In contrast, de Bont et al. (world patent WO2013081456) have explored partial GPD inactivation.

With a consumption of 0.046 g acetate per g glucose, strain

M9843 reached 16% of the maximal theoretical uptake stoichiometry. This suggests that there are still many opportunities to debottleneck the pathway by optimizing enzymes and their expression levels. However, since the pathway to convert acetate to ethanol requires an ATP investment, there is a trade-off between acetate consumption and cellular growth. As such, the optimal level of acetate consumption will likely have to be determined case by case, depending on the exact metabolic pathways used, the availability of sugars, acetate, and other cosubstrates in the medium, inhibitor concentrations, the fermentation pH, and the rate at which biomass needs to be produced during the fermentation.

In conclusion, the introduction of *E. histolytica* NADPH-ADH, combined with overexpression of *ACS2* and *ZWF1*, improved acetate uptake in flushed bottles almost 3-fold compared to that of our *Gpd*⁻ Ba-*adhE* strain: from 0.017 ± 0.000 g acetate (g glucose)⁻¹ with M6571 to 0.046 ± 0.001 g acetate (g glucose)⁻¹ with M9843. Our final M9843 strain consumed 5.3 g liter⁻¹ acetate during anaerobic fermentation of 114 g liter⁻¹ glucose, producing 3.4 g liter⁻¹ more ethanol than the wild-type M2390 strain, a 7% increase. Apart from increasing yields, converting acetate to ethanol can further improve the economics of second-generation biofuel production by reducing the substrate toxicity, improving the strain tolerance, and reducing the need for pH control. This metabolic pathway is therefore of high interest to the biofuel industry.

ACKNOWLEDGMENTS

This work was supported by the BioEnergy Science Center (BESC). The BioEnergy Science Center is a U.S. Department of Energy Bioenergy Research Center supported by the Office of Biological and Environmental Research in the DOE Office of Science.

We thank Victor Guadalupe Medina for providing additional details regarding his publications.

B.M.H., S.H., D.A.A., and T.F.B. designed and built strains. S.F.C. performed fermentations. C.S. and E.W. designed and performed enzyme assays. A.C.F. participated in the design and coordination of the study. R.M.Z. conceived of the study, designed and built strains, performed fermentations and enzyme assays, and wrote the manuscript. All authors read and approved the final manuscript.

A patent application on the reported findings has been filed by Mascoma LLC (R. M. Zelle, A. J. Shaw, and J. P. van Dijken, May 2014, world patent application WO2014074895).

REFERENCES

1. Alternative Fuels Data Center. 2015. Global ethanol production. Alternative Fuels Data Center, Washington, DC. <http://www.afdc.energy.gov/data/10331>.
2. Schwartz K, Wenger JW, Dunn B, Sherlock G. 2012. *APJ1* and *GRE3* homologs work in concert to allow growth in xylose in a natural *Saccharomyces sensu stricto* hybrid yeast. *Genetics* 191:621–632. <http://dx.doi.org/10.1534/genetics.112.140053>.
3. Wisselink HW, Toirkens MJ, del Rosario Franco Berriel M, Winkler AA, van Dijken JP, Pronk JT, van Maris AJA. 2007. Engineering of *Saccharomyces cerevisiae* for efficient anaerobic alcoholic fermentation of L-arabinose. *Appl Environ Microbiol* 73:4881–4891. <http://dx.doi.org/10.1128/AEM.00177-07>.
4. Klinker HB, Thomsen AB, Ahring BK. 2004. Inhibition of ethanol-producing yeast and bacteria by degradation products produced during pre-treatment of biomass. *Appl Microbiol Biotechnol* 66:10–26. <http://dx.doi.org/10.1007/s00253-004-1642-2>.
5. Palmqvist E, Hahn-Hägerdal B. 2000. Fermentation of lignocellulosic hydrolysates. I. Inhibition and detoxification. *Bioresour Technol* 74:17–24. [http://dx.doi.org/10.1016/S0960-8524\(99\)00160-1](http://dx.doi.org/10.1016/S0960-8524(99)00160-1).
6. Palmqvist E, Hahn-Hägerdal B. 2000. Fermentation of lignocellulosic

- hydrolysates. II. Inhibitors and mechanisms of inhibition. *Bioresour Technol* 74:25–33. [http://dx.doi.org/10.1016/S0960-8524\(99\)00161-3](http://dx.doi.org/10.1016/S0960-8524(99)00161-3).
7. Becker J, Boles E. 2003. A modified *Saccharomyces cerevisiae* strain that consumes L-arabinose and produces ethanol. *Appl Environ Microbiol* 69: 4144–4150. <http://dx.doi.org/10.1128/AEM.69.7.4144-4150.2003>.
 8. Kim SR, Park Y-C, Jin Y-S, Seo J-H. 2013. Strain engineering of *Saccharomyces cerevisiae* for enhanced xylose metabolism. *Biotechnol Adv* 31: 851–861. <http://dx.doi.org/10.1016/j.biotechadv.2013.03.004>.
 9. Kuyper M, Winkler AA, van Dijken JP, Pronk JT. 2004. Minimal metabolic engineering of *Saccharomyces cerevisiae* for efficient anaerobic xylose fermentation: a proof of principle. *FEMS Yeast Res* 4:655–664. <http://dx.doi.org/10.1016/j.femsysr.2004.01.003>.
 10. Gorsich SW, Dien BS, Nichols NN, Slininger PJ, Liu ZL, Skory CD. 2006. Tolerance to furfural-induced stress is associated with pentose phosphate pathway genes *ZWF1*, *GND1*, *RPE1*, and *TKL1* in *Saccharomyces cerevisiae*. *Appl Microbiol Biotechnol* 71:339–349. <http://dx.doi.org/10.1007/s00253-005-0142-3>.
 11. Jayakody LN, Horie K, Hayashi N, Kitagaki H. 2013. Engineering redox cofactor utilization for detoxification of glycolaldehyde, a key inhibitor of bioethanol production, in yeast *Saccharomyces cerevisiae*. *Appl Microbiol Biotechnol* 97:6589–6600. <http://dx.doi.org/10.1007/s00253-013-4997-4>.
 12. Liu ZL, Moon J. 2009. A novel NADPH-dependent aldehyde reductase gene from *Saccharomyces cerevisiae* NRRL Y-12632 involved in the detoxification of aldehyde inhibitors derived from lignocellulosic biomass conversion. *Gene* 446:1–10. <http://dx.doi.org/10.1016/j.gene.2009.06.018>.
 13. Wright J, Bellissimi E, de Hulster E, Wagner A, Pronk JT, van Maris AJA. 2011. Batch and continuous culture-based selection strategies for acetic acid tolerance in xylose-fermenting *Saccharomyces cerevisiae*. *FEMS Yeast Res* 11:299–306. <http://dx.doi.org/10.1111/j.1567-1364.2011.00719.x>.
 14. Palmqvist E, Hahn-Hägerdal B, Galbe M, Zacchi G. 1996. The effect of water-soluble inhibitors from steam-pretreated willow on enzymatic hydrolysis and ethanol fermentation. *Enzyme Microb Technol* 19:470–476. [http://dx.doi.org/10.1016/S0141-0229\(95\)00234-0](http://dx.doi.org/10.1016/S0141-0229(95)00234-0).
 15. Bellissimi E, van Dijken JP, Pronk JT, van Maris AJA. 2009. Effects of acetic acid on the kinetics of xylose fermentation by an engineered, xylose-isomerase-based *Saccharomyces cerevisiae* strain. *FEMS Yeast Res* 9:358–364. <http://dx.doi.org/10.1111/j.1567-1364.2009.00487.x>.
 16. Giannattasio S, Guaragnella N, Ždravčević M, Marra E. 2013. Molecular mechanisms of *Saccharomyces cerevisiae* stress adaptation and programmed cell death in response to acetic acid. *Front Microb* 4:33. <http://dx.doi.org/10.3389/fmicb.2013.00033>.
 17. Taherzadeh MJ, Niklasson C, Lidén G. 1997. Acetic acid—friend or foe in anaerobic batch conversion of glucose to ethanol by *Saccharomyces cerevisiae*? *Chem Eng Sci* 52:2653–2659. [http://dx.doi.org/10.1016/S0009-2509\(97\)00080-8](http://dx.doi.org/10.1016/S0009-2509(97)00080-8).
 18. Guadalupe Medina V, Almering MJH, van Maris AJA, Pronk JT. 2010. Elimination of glycerol production in anaerobic cultures of a *Saccharomyces cerevisiae* strain engineered to use acetic acid as an electron acceptor. *Appl Environ Microbiol* 76:190–195. <http://dx.doi.org/10.1128/AEM.01772-09>.
 19. de Smidt O, du Preez JC, Albertyn J. 2008. The alcohol dehydrogenases of *Saccharomyces cerevisiae*: a comprehensive review. *FEMS Yeast Res* 8:967–978. <http://dx.doi.org/10.1111/j.1567-1364.2008.00387.x>.
 20. van Dijken JP, Scheffers WA. 1986. Redox balances in the metabolism of sugars by yeasts. *FEMS Microbiol Lett* 32:199–224. <http://dx.doi.org/10.1111/j.1574-6968.1986.tb01194.x>.
 21. Verduyn C, Postma E, Scheffers WA, van Dijken JP. 1990. Physiology of *Saccharomyces cerevisiae* in anaerobic glucose-limited chemostat cultures. *J Gen Microbiol* 136:395–403. <http://dx.doi.org/10.1099/00221287-136-3-395>.
 22. Celton M, Goelzer A, Camarasa C, Fromion V, Dequin S. 2012. A constraint-based model analysis of the metabolic consequences of increased NADPH oxidation in *Saccharomyces cerevisiae*. *Metab Eng* 14: 366–379. <http://dx.doi.org/10.1016/j.ymben.2012.03.008>.
 23. Guadalupe Medina V, Metz B, Oud B, van der Graaf CM, Mans R, Pronk JT, van Maris AJA. 2014. Evolutionary engineering of a glycerol-3-phosphate dehydrogenase-negative, acetate-reducing *Saccharomyces cerevisiae* strain enables anaerobic growth at high glucose concentrations. *Microb Biotechnol* 7:44–53. <http://dx.doi.org/10.1111/1751-7915.12080>.
 24. Wei N, Quarterman J, Kim SR, Cate JHD, Jin Y-S. 2013. Enhanced biofuel production through coupled acetic acid and xylose consumption by engineered yeast. *Nat Commun* 4:2580. <http://dx.doi.org/10.1038/ncomms3580>.
 25. Walfridsson M, Anderlund M, Bao X, Hahn-Hägerdal B. 1997. Expression of different levels of enzymes from the *Pichia stipitis* *XYL1* and *XYL2* genes in *Saccharomyces cerevisiae* and its effects on product formation during xylose utilisation. *Appl Microbiol Biotechnol* 48:218–224. <http://dx.doi.org/10.1007/s002530051041>.
 26. Watanabe S, Saleh AA, Pack SP, Annaluru N, Kodaki T, Makino K. 2007. Ethanol production from xylose by recombinant *Saccharomyces cerevisiae* expressing protein engineered NADP⁺-dependent xylitol dehydrogenase. *J Biotechnol* 130:316–319. <http://dx.doi.org/10.1016/j.jbiotec.2007.04.019>.
 27. Zhou H, Cheng J, Wang BL, Fink GR, Stephanopoulos G. 2012. Xylose isomerase overexpression along with engineering of the pentose phosphate pathway and evolutionary engineering enable rapid xylose utilization and ethanol production by *Saccharomyces cerevisiae*. *Metab Eng* 14: 611–622. <http://dx.doi.org/10.1016/j.ymben.2012.07.011>.
 28. Zhang L, Tang Y, Guo Z, Shi G. 2013. Engineering of the glycerol decomposition pathway and cofactor regulation in an industrial yeast improves ethanol production. *J Ind Microbiol Biotechnol* 40:1153–1160. <http://dx.doi.org/10.1007/s10295-013-1311-5>.
 29. Verduyn C, Postma E, Scheffers WA, van Dijken JP. 1992. Effect of benzoic acid on metabolic fluxes in yeasts: a continuous-culture study on the regulation of respiration and alcoholic fermentation. *Yeast* 8:501–517. <http://dx.doi.org/10.1002/yea.320080703>.
 30. Postma E, Verduyn C, Scheffers WA, van Dijken JP. 1989. Enzymic analysis of the Crabtree effect in glucose-limited chemostat cultures of *Saccharomyces cerevisiae*. *Appl Environ Microbiol* 55:468–477.
 31. Kumar A, Shen PS, Descoteaux S, Pohl J, Bailey G, Samuelson J. 1992. Cloning and expression of an NADP⁺-dependent alcohol dehydrogenase gene of *Entamoeba histolytica*. *Proc Natl Acad Sci U S A* 89:10188–10192. <http://dx.doi.org/10.1073/pnas.89.21.10188>.
 32. Grabowska D, Chelstowska A. 2003. The *ALD6* gene product is indispensable for providing NADPH in yeast cells lacking glucose-6-phosphate dehydrogenase activity. *J Biol Chem* 278:13984–13988. <http://dx.doi.org/10.1074/jbc.M210076200>.
 33. Minard KI, McAlister-Henn L. 2005. Sources of NADPH in yeast vary with carbon source. *J Biol Chem* 280:39890–39896. <http://dx.doi.org/10.1074/jbc.M509461200>.
 34. Nogue I, Johnston M. 1990. Isolation and characterization of the *ZWF1* gene of *Saccharomyces cerevisiae*, encoding glucose-6-phosphate dehydrogenase. *Gene* 96:161–169. [http://dx.doi.org/10.1016/0378-1119\(90\)90248-P](http://dx.doi.org/10.1016/0378-1119(90)90248-P).
 35. Izawa S, Maeda K, Miki T, Mano J, Inoue Y, Kimura A. 1998. Importance of glucose-6-phosphate dehydrogenase in the adaptive response to hydrogen peroxide in *Saccharomyces cerevisiae*. *Biochem J* 330:811–817. <http://dx.doi.org/10.1042/bj3300811>.
 36. Park S-E, Koo HM, Park YK, Park SM, Park JC, Lee O-K, Park Y-C, Seo J-H. 2011. Expression of aldehyde dehydrogenase 6 reduces inhibitory effect of furan derivatives on cell growth and ethanol production in *Saccharomyces cerevisiae*. *Bioresour Technol* 102:6033–6038. <http://dx.doi.org/10.1016/j.biortech.2011.02.101>.
 37. Kwon D-H, Kim M-D, Lee T-H, Oh Y-J, Ryu Y-W, Seo J-H. 2006. Elevation of glucose 6-phosphate dehydrogenase activity increases xylitol production in recombinant *Saccharomyces cerevisiae*. *J Mol Catal B Enzym* 43:86–89. <http://dx.doi.org/10.1016/j.molcatb.2006.06.014>.
 38. Oh Y-J, Lee T-H, Lee S-H, Oh E-J, Ryu Y-W, Kim M-D, Seo J-H. 2007. Dual modulation of glucose 6-phosphate metabolism to increase NADPH-dependent xylitol production in recombinant *Saccharomyces cerevisiae*. *J Mol Catal B Enzym* 47:37–42. <http://dx.doi.org/10.1016/j.molcatb.2007.03.011>.
 39. Henry SA, Kohlwein SD, Carman GM. 2012. Metabolism and regulation of glycerolipids in the yeast *Saccharomyces cerevisiae*. *Genetics* 190:317–349. <http://dx.doi.org/10.1534/genetics.111.130286>.
 40. Chen Y, Daviet L, Schalk M, Siewers V, Nielsen J. 2013. Establishing a platform cell factory through engineering of yeast acetyl-CoA metabolism. *Metab Eng* 15:48–54. <http://dx.doi.org/10.1016/j.ymben.2012.11.002>.
 41. Kocharin K, Chen Y, Siewers V, Nielsen J. 2012. Engineering of acetyl-CoA metabolism for the improved production of polyhydroxybutyrate in *Saccharomyces cerevisiae*. *AMB Express* 2:52. <http://dx.doi.org/10.1186/2191-0855-2-52>.
 42. Shiba Y, Paradise EM, Kirby J, Ro D-K, Keasling JD. 2007. Engineering of the pyruvate dehydrogenase bypass in *Saccharomyces cerevisiae* for

- high-level production of isoprenoids. *Metab Eng* 9:160–168. <http://dx.doi.org/10.1016/j.ymben.2006.10.005>.
43. Oh E-J, Bae Y-H, Kim K-H, Park Y-C, Seo J-H. 2012. Effects of over-expression of acetaldehyde dehydrogenase 6 and acetyl-CoA synthetase 1 on xylitol production in recombinant *Saccharomyces cerevisiae*. *Biocatal Agric Biotechnol* 1:15–19. <http://dx.doi.org/10.1016/j.bcab.2011.08.011>.
 44. de Jong-Gubbels P, van den Berg MA, Steensma HY, van Dijken JP, Pronk JT. 1997. The *Saccharomyces cerevisiae* acetyl-coenzyme A synthetase encoded by the *ACS1* gene, but not the *ACS2*-encoded enzyme, is subject to glucose catabolite inactivation. *FEMS Microbiol Lett* 153:75–81. <http://dx.doi.org/10.1111/j.1574-6968.1997.tb10466.x>.
 45. King ZA, Feist AM. 2014. Optimal cofactor swapping can increase the theoretical yield for chemical production in *Escherichia coli* and *Saccharomyces cerevisiae*. *Metab Eng* 24:117–128. <http://dx.doi.org/10.1016/j.ymben.2014.05.009>.
 46. Ansell R, Granath K, Hohmann S, Thevelein JM, Adler L. 1997. The two isoenzymes for yeast NAD⁺-dependent glycerol 3-phosphate dehydrogenase encoded by *GPD1* and *GPD2* have distinct roles in osmoadaptation and redox regulation. *EMBO J* 16:2179–2187. <http://dx.doi.org/10.1093/emboj/16.9.2179>.
 47. Hubmann G, Guillouet S, Nevoigt E. 2011. Gpd1 and Gpd2 fine-tuning for sustainable reduction of glycerol formation in *Saccharomyces cerevisiae*. *Appl Environ Microbiol* 77:5857–5867. <http://dx.doi.org/10.1128/AEM.05338-11>.
 48. Pagliardini J, Hubmann G, Alfenore S, Nevoigt E, Bideaux C, Guillouet SE. 2013. The metabolic costs of improving ethanol yield by reducing glycerol formation capacity under anaerobic conditions in *Saccharomyces cerevisiae*. *Microb Cell Fact* 12:29. <http://dx.doi.org/10.1186/1475-2859-12-29>.
 49. Flamholz A, Noor E, Bar-Even A, Milo R. 2012. eQuilibrator—the biochemical thermodynamics calculator. *Nucleic Acids Res* 40:D770–D775. <http://dx.doi.org/10.1093/nar/gkr874>.